Spectrum Sensing of OFDM Signals in the Presence of Carrier Frequency Offset

Weiyang Xu, Wei Xiang, *Senior Member, IEEE*,
Maged Elkashlan, *Member, IEEE,* and Hani Mehrpouyan, *Member, IEEE*

***Abstract*—This paper addresses the important issue of detecting orthogonal frequency-division multiplexing (OFDM) signals in the presence of carrier frequency offset (CFO). The proposed algorithm utilizes the characteristics of the covariance matrix of the discrete Fourier transform of the input signal to the detector to determine the presence of the primary user's signal. This algorithm can be exploited to differentiate OFDM signals from the noise through the proposal of a new decision metric, which measures the off-diagonal elements of the input signal's covariance matrix. The decision threshold subject to a given probability of false alarm is derived, while performance analysis is carried out to demonstrate the potential of the proposed algorithm. Finally, simulation results are presented to validate the effectiveness of the proposed sensing method in comparison with other existing approaches.**

***Index Terms*—OFDM, cognitive radio, spectrum sensing, covariance matrix, carrier frequency offset.**

I. Introduction

SENSING the presence of the primary user's signal is one of the most critical and challenging tasks in cognitive radio (CR). Existing algorithms can be generally classified into methods of matched-filter detection, energy detection, and feature detection [1]. Recently, a new detection method has been proposed, which uses eigenvalues of the signal covariance matrix [2]. This approach is shown to perform well when the signals to be detected are mutually correlated [3].

Orthogonal frequency-division multiplexing (OFDM) has been considered as a promising candidate for implementing the physical layer of CR due to its capability of transmitting over non-contiguous frequency bands. However, sensing OFDM signals proves to be more challenging thanks to its multi-carrier characteristics. Currently, existing schemes make use of either the cyclic prefix (CP) [4][5], or pilot tones in OFDM symbols [6][7]. In [4], Lei $et\ al.$ introduced a decision metric with the aid of the CP, and derived the generalized likelihood ratio test (GLRT) for this decision metric. Bokharaiee $et\ al.$ proposed a constrained GLRT by using the multipath correlation amongst the primary signals [5]. Unfortunately, the performance of the CP-based schemes will degrade substantially if the length of the CP is reduced to enhance spectral efficiency. Relying on pilot tones, a detection scheme that utilizes the cross-correlation amongst the time-domain symbols was suggested in [6]. Moreover, a pilot-aided second-order cyclostationary detection algorithm was derived in [7], demonstrating a superior performance. However, since pilots are usually pseudo-randomly coded and uniquely dedicated to the primary transmission, it is nontrivial or even impossible for cognitive users to obtain this information accurately. More importantly, all the aforementioned methods fail to take into account the carrier frequency offset (CFO). In general, solutions to tackle the CFO can be divided into two categories. The first one estimates and compensates for the CFO errors before spectrum sensing. For example, Chen $et\ al.$ employed the CP-based synchronization method to compensate for the CFO [8]. However, the estimation accuracy degrades severely because the detector often works in highly noisy environments. The second one exploits hybrid domain signal processing algorithms to design spectrum sensing schemes robust to the CFO, but pilot symbols are required to be perfectly known to the cognitive users [9].

In this paper, we focus on the detection of OFDM signals in CR systems in consideration of the CFO. The major contributions of this paper are summarized as follows:

1) A new decision metric robust to the CFO is introduced, which is based on the covariance matrix of the discrete Fourier transform (DFT) of the detector's input vector;
2) A decision threshold is computed according to the required probability of false alarm. A performance analysis concerning the detection probability and computational complexity of the proposed method is also carried out.

The remainder of this paper is organized as follows. Section II describes the OFDM-based CR system model. A new decision metric is proposed based on the covariance matrix in Section III. The detection probability and complexity of the proposed detector are analyzed in Section IV. Section V and VI present the numerical results and conclude this paper, respectively.

$Notation$: Lower and upper case symbols are used for time and frequency domain signals, respectively. $(\cdot)^*$, $(\cdot)^T$ and $(\cdot)^H$ denote conjugate, transpose, and conjugate transpose, respectively. $\mathbf{F}_N$, $\mathbf{1}_N$ and $\mathbf{I}_N$ indicate the DFT matrix, the

Weiyang Xu is with the College of Communication Engineering, Chongqing University, Chongqing 400044, P. R. China (e-mail: weiyangxu@cqu.edu.cn).

Wei Xiang is with the School of Mechanical and Electrical Engineering, University of Southern Queensland, Toowoomba, QLD 4350, Australia (e-mail: wei.xiang@usq.edu.au).

Maged Elkashlan is with the School of Electronic Engineering and Computer Science, Queen Mary University of London, London E1 4NS, UK (email: maged.elkashlan@qmul.ac.uk).

Hani Mehrpouyan is with the Department of Electrical and Computer Engineering, Boise State University, Boise, Idaho 83725, USA (email: hani.mehr@ieee.org).

matrix of ones, and the identity matrix, respectively, all of size $N \times N$. $Q(x) = \frac{2}{\sqrt{\pi}} \int_x^\infty e^{-t^2} \mathrm{d}t$ is the complementary error function. At last, $\mathrm{E}[\cdot]$, $\|\cdot\|_{L_1}$ and $\odot$ are the expectation, L_1 norm and Hadamard product operators, respectively.

II. System Model and Problem Formulation

At the transmitter side, the samples of the i^{th} OFDM symbol is given by

$$x_{i,n} = \frac{1}{\sqrt{N}} \sum_{k=0}^{N-1} X_{i,k} e^{j\frac{2\pi}{N}nk}, \quad -N_g \le n \le N-1, \tag{1}$$

where $X_{i,k}$, which is assumed to have unit variance, represents the symbol modulating the k^{th} subcarrier, and N_g is the length of the CP. The resultant baseband signal is up-converted to passband and propagates through the wireless environment. There usually exists the CFO in the received signal because of the mismatch between the transmitter and receiver's local oscillators or the Doppler effect. Therefore, the baseband discrete-time signal can be written as

$$r_{i,n} = e^{j\frac{2\pi}{N}n\varepsilon} \sum_{l=0}^{L-1} h_l x_{i,n-l} + w_{i,n}, \tag{2}$$

where ε is the normalized CFO, h_l indicates the impulse response of the l^{th} channel tap, L is the number of taps, $w_{i,n}$ is the Gaussian noise with zero mean and variance σ_n^2. On the other hand, when no primary users is present, the received signal is simply equal to $w_{i,n}$.

Thus, sensing OFDM signals can be formulated as a binary hypothesis testing problem

$$\begin{aligned} \mathcal{H}_0 &: r_{i,n} = w_{i,n} \\ \mathcal{H}_1 &: r_{i,n} = d_{i,n} + w_{i,n}, \end{aligned} \tag{3}$$

where $d_{i,n}$ is the received primary user's signal, $\mathcal{H}_0$ and $\mathcal{H}_1$ indicate the absence and presence of the primary user, respectively. Since cognitive users may not have access to training symbols or pilots, it is unrealistic to assume perfect synchronization. As a result, the proposed sensing method should be designed to be resilient to the CFO.

III. Covariance Matrix Based Spectrum Sensing Algorithm

A. Properties of the Signal Covariance Matrix

The different properties of the signal covariance matrix in the frequency domain under $\mathcal{H}_0$ and $\mathcal{H}_1$ constitute the basis of our method. Let $\mathbf{w}_i \triangleq [w_{i,0}, ..., w_{i,N-1}]^T$ be the input vector under $\mathcal{H}_0$, it is readily shown the covariance matrix of $\mathbf{W}_i = \mathbf{F}_N \mathbf{w}_i$ is $\sigma_n^2 \mathbf{I}_N$.

In the presence of primary user's signal, let $\mathbf{r}_i \triangleq [r_{i,0}, ..., r_{i,N-1}]^T$ be the N-point input vector of the detector after discarding the CP, then the DFT of $\mathbf{r}_i$ is given by

$$\mathbf{Y}_i = \mathbf{F}_N \mathbf{r}_i = \mathbf{F}_N \boldsymbol{\Phi}(\varepsilon) \mathbf{F}_N^H \mathbf{H} \mathbf{X}_i + \mathbf{W}_i, \tag{4}$$

where

$$\begin{aligned} \mathbf{Y}_i &\triangleq [Y_{i,0}, ..., Y_{i,N-1}]^T, \\ \mathbf{X}_i &\triangleq [X_{i,0}, ..., X_{i,N-1}]^T, \\ \mathbf{H} &\triangleq \text{diag}\{H_{i,0}, ..., H_{i,N-1}\}, \\ \Phi(\varepsilon) &\triangleq \text{diag}\left\{1, e^{j2\pi\varepsilon/N}, ..., e^{j2\pi(N-1)\varepsilon/N}\right\}. \end{aligned}$$

Here, $H_{i,k} = \frac{1}{\sqrt{N}} \sum_{l=0}^{L-1} h_l e^{-j2\pi kl/N}$, for $0 \le k \le N-1$, denotes the frequency response of the k^{th} subcarrier. The channel is assumed to be constant during spectrum sensing. Therefore, the covariance matrix of $\mathbf{Y}_i$ can be represented by

$$\mathbf{R} = \mathbf{F}_N^H \boldsymbol{\Phi}(\varepsilon) \mathbf{F}_N \mathbf{H} \mathbf{H}^H \mathbf{F}_N^H \boldsymbol{\Phi}^*(\varepsilon) \mathbf{F}_N + \sigma_n^2 \mathbf{I}_N. \tag{5}$$

For better understanding, the k^{th} element of $\mathbf{Y}_i$ is

$$Y_{i,k} = \sum_{t=0}^{N-1} I_{t-k}^{\varepsilon} X_{i,t} H_{i,t} + W_{i,k}, \tag{6}$$

where

$$I_n^{\varepsilon} = \frac{\sin(\pi\varepsilon)}{N \sin\left(\frac{\pi}{N}(\varepsilon + n)\right)} \exp\left(j\frac{\pi}{N}((N-1)\varepsilon - n)\right).$$

Therefore, the $(p,q)^{th}$ entry of the covariance matrix can be written as

$$\mathbf{R}(p,q) = \begin{cases} \sum_{t=0}^{N-1} \left|I_{t-p}^{\varepsilon} H_{i,t}\right|^2 + \sigma_n^2, & p = q \\ \sum_{t=0}^{N-1} I_{t-p}^{\varepsilon} I_{t-q}^{\varepsilon\,*} |H_{i,t}|^2. & p \ne q \end{cases} \tag{7}$$

It is evident that $\mathbf{R}$ is non-diagonal due to the intercarrier interference (ICI) among subcarriers. However, when ε denotes the integer CFO, it can be derived that $\sum_{t=0}^{N-1} I_{t-p}^{\varepsilon} I_{t-q}^{\varepsilon\,*} |H_{i,t}|^2 = 0$. Hence, the covariance matrix is still diagonal under $\mathcal{H}_1$.

B. Proposed Spectrum Sensing Algorithm

Based on the above discussions, it can be concluded that if the detector's input contains the primary user's signal contaminated by the CFO, the covariance matrix is not diagonal except when ε is an integer, as opposed to hypothesis $\mathcal{H}_0$ where only the noise is present. Hence, this property can be exploited to detect the primary user's signal by comparing the off-diagonal power of the covariance matrix with a preset threshold. Since $\mathbf{R}$ cannot be obtained practically, we resort to the sample covariance matrix $\hat{\mathbf{R}}$, which is computed by

$$\hat{\mathbf{R}} = \frac{1}{M} \sum_{i=1}^{M} \mathbf{Y}_i \mathbf{Y}_i^H, \tag{8}$$

where M indicates the number of OFDM symbols. Thus, the decision metric can be written as

$$\zeta = \frac{\left\|\hat{\mathbf{R}} \odot (\mathbf{1}_N - \mathbf{I}_N)\right\|_{L_1}}{\sqrt{N^2 - N}}, \tag{9}$$

which is essentially the sum of magnitudes of $(N^2 - N)$ non-diagonal elements of $\hat{\mathbf{R}}$, and the denominator is the normalizing factor. Since γ is selected with respect to the P_{fa}, the probability distribution function (PDF) under $\mathcal{H}_0$ needs to be fully established.

Lemma 1: It can be shown that if M is sufficiently large, the decision metric ζ in (9), can be approximated as a sum of $(N^2-N)/2$ *independent and identically distributed* (i.i.d.) Rayleigh variables under $\mathcal{H}_0$. (Please refer to Appendix A for detailed derivation.)

Based on Lemma 1, there is no closed-form expression for the PDF of ζ. Hence, we resort to a simple approximation outlined in [10]. Let $K=\left(N^2-N\right)/2$, the PDF of ζ can be approximated using the central limit theorem (CLT) (For detailed derivation, please refer to Appendix A.)

$$p\left(\zeta|\mathcal{H}_0\right)\approx\frac{1}{\sqrt{2\pi}}e^{-\frac{1}{2}\left(\frac{\zeta-\mu_{\mathcal{H}_0}\sqrt{K}}{\sigma_{\mathcal{H}_0}}\right)^2}, \tag{10}$$

where

$$\mu_{\mathcal{H}_0}=\sqrt{\frac{\pi}{4M}}\sigma_n^2, \qquad \sigma_{\mathcal{H}_0}^2=\left(1-\frac{\pi}{4}\right)\frac{\sigma_n^4}{M}.$$

Given a preset P_{fa}, the threshold, γ, is constrained by [11]

$$P_{fa}=\int_{\gamma}^{\infty}p\left(\zeta|\mathcal{H}_0\right)d\zeta. \tag{11}$$

By substituting (10) into (11), we can calculate the decision threshold using

$$\gamma=Q^{-1}\left(\frac{2P_{fa}}{\sigma_{\mathcal{H}_0}}\right)\sigma_{\mathcal{H}_0}+\mu_{\mathcal{H}_0}\sqrt{K}. \tag{12}$$

(12) shows γ relates to M, N, P_{fa}, and noise variance σ_n^2. Since we can choose the values of M, N, and P_{fa} before sensing, the only unknown is σ_n^2. To tackle this issue, a real-time noise power estimation scheme is exploited [12]. In OFDM, there are a few null subcarriers used as the guard band. So the received signal power on such a null subcarrier is close to the noise power if there is no interference or out of band signal intrusion on the subcarrier. As the index of null subcarriers is available to cognitive users, we can choose these subcarriers for noise power estimation. With the estimate $\hat{\sigma}_n^2$, γ can be obtained before making a decision.

C. Spectrum Sensing with CFO Being an Integer Multiple of Subcarrier Spacing

For the complete study, the applicability of the our spectrum sensing algorithm in the presence of an integer CFO will be analyzed in this section.

Lemma 2: The proposed scheme works when the CFO is an integer multiple of subcarrier spacing. In this scenario, it is shown that the PDF of the decision metric can be represented as (For detailed derivation, please refer to Appendix A.)

$$p_{\mathrm{IFO}}\left(\zeta|\mathcal{H}_1\right)\approx\frac{1}{\sqrt{2\pi}}e^{-\frac{1}{2}\left(\frac{\zeta-\mu_{\mathcal{H}_1}\sqrt{K}}{\sigma_{\mathcal{H}_1}}\right)^2}, \tag{13}$$

where

$$\mu_{\mathrm{IFO},\mathcal{H}_1}=\sqrt{\frac{\pi}{4M}\left(\sigma_n^4+2\sigma_n^2\sigma_H^2\right)},$$
$$\sigma_{\mathrm{IFO},\mathcal{H}_1}^2=\left(1-\frac{\pi}{4}\right)\frac{\left(\sigma_n^4+2\sigma_n^2\sigma_H^2\right)}{M},$$

with subscript "IFO" denoting the scenario with an integer CFO and σ_H^2 being the variance of the channel frequency response. The proposed algorithm is expected to differentiate the primary user's signal from noise because $\mu_{\mathrm{IFO},\mathcal{H}_1}>\mu_{\mathcal{H}_0}$. Thus, (13) indicates that our scheme can detect the primary user's signal even in the presence of CFO that is an integer multiple of the subcarrier spacing. Note that the CFO-free scenario is a special case of Lemma 2 when $\varepsilon=0$. In fact, although the proposed algorithm is designed to tackle the spectrum sensing with the CFO, its applicability in the absence of this error is also shown.

D. Timing Issue

The impact of timing offsets on our scheme needs to be addressed. Since $w_{i,n}$ is immune to timing offsets, the covariance matrix is still diagonal under $\mathcal{H}_0$. Under $\mathcal{H}_1$, the DFT window contains data from two consecutive OFDM symbols when the timing offset is outside the ISI-free region [13]. As a result, the independence among subcarriers is destroyed such that the covariance matrix becomes non-diagonal. According to our former analysis, the proposed algorithm works in this situation. The covariance matrix is diagonal if the timing offset resides in the ISI-free region. It can be shown that the proposed method in this scenario is applicable in a way similar to that in Section III. C. Therefore, it is concluded that the proposed scheme still works in the presence of timing offsets, which further enhances the practicality of the algorithm.

IV. Performance Analysis and Discussion

A. Probability of Detection and Complexity Analysis

The PDF of the decision metric under $\mathcal{H}_1$ is unavailable since it depends on the unknown CFO. However, without any loss of generality, we can assume that the frequency offset is evenly distributed in a certain range and can be integrated out in order to conduct performance analysis concerning the P_d. Here we assume the CFO is evenly distributed over $(-0,5,0.5]$ [9].

It is proved that ζ in this scenario can be approximated as the sum of Ricean variables. The corresponding PDF is represented as (Please refer to Appendix B for detailed derivation.)

$$p\left(\zeta|\mathcal{H}_1\right)\approx\frac{1}{\sqrt{2\pi}}e^{-\frac{1}{2}\left(\frac{\zeta-\mu_{\mathcal{H}_1}\sqrt{K}}{\sigma_{\mathcal{H}_1}}\right)^2}, \tag{14}$$

where

$$\mu_{\mathcal{H}_1}=L_{1/2}\left(-\nu^2\right)\sqrt{\frac{\pi}{4M}}\sigma_n^2,$$
$$\sigma_{\mathcal{H}_1}^2=\frac{\sigma_n^4}{M}+\frac{\sigma_n^4\nu^2}{M}-\frac{\pi\sigma_n^4}{4M}L_{1/2}^2\left(-\nu^2\right),$$
$$\nu=\frac{4\pi^2\sigma_n^2N\sqrt{M}\sigma_H^2}{\left(\Gamma+\psi\left(N\right)\right)^2+\psi\left(1,N\right)-\pi^2/6}.$$

Here, $L_{1/2}\left(x\right)=e^{x/2}\left[\left(1-x\right)J_0\left(-x/2\right)-xJ_1\left(-x/2\right)\right]$ represents the Laguerre polynomial with $J_p\left(\cdot\right)$ being the p^{th} order modified Bessel function of the first kind, Γ is the

TABLE I
COMPARISON OF COMPLEX MULTIPLICATIONS AMONG SENSING ALGORITHMS

Algorithms	Number of complex multiplications
Proposed scheme	$MN\log_2 N/2 + MN^2$
Method in [4]	$M\left(N+N_g\right)^2$
Method in [6]	M^2N/z
Method in [8]	$MN_g\left(N+N_g\right)+MN\log_2\left(N\right)+M^2N/2z^2$

Euler-Mascheroni constant, $\psi\left(\cdot\right)$ and $\psi\left(1,\cdot\right)$ denote the logarithmic derivatives of the gamma and trigamma functions, respectively. The fact that $\mu_{\mathcal{H}_1}$ is always larger than $\mu_{\mathcal{H}_0}$ in (10), which follows from $L_{1/2}\left(-\nu^2\right)>1$, i.e., the argument of monotonically decreasing function $L_{1/2}\left(\cdot\right)$ is negative and $L_{1/2}\left(0\right)=1$, lays the foundation for the proposed spectrum sensing scheme.

Given the PDF under $\mathcal{H}_1$, the probability of detection P_d is calculated by $\Pr\left\{\zeta>\gamma;\mathcal{H}_1\right\}$, i.e.,

$$P_d=\frac{1}{2}Q\left(\frac{\gamma-\mu_{\mathcal{H}_1}\sqrt{K}}{\sqrt{2}\sigma_{\mathcal{H}_1}}\right). \tag{15}$$

Moreover, P_d can be rewritten by substituting (12) into (15)

$$P_d=\frac{1}{2}Q\left(\frac{Q^{-1}\left(2P_{fa}/\sigma_{\mathcal{H}_0}\right)\sigma_{\mathcal{H}_0}-\left(\mu_{\mathcal{H}_1}-\mu_{\mathcal{H}_0}\right)\sqrt{K}}{\sqrt{2}\sigma_{\mathcal{H}_1}}\right). \tag{16}$$

It can be shown that P_d is a monotonically increasing function of both M and N, which means larger M and N values lead to higher detection accuracy.

As for the complexity analysis, the number of complex multiplications is only considered since they are computationally most intensive. In order to have a deep insight, we include recently proposed methods in [4], [6], [8] for comparison. The results are listed in Table I.

B. Relation with Eigenvalue-based Algorithm in [2]

Among existing methods, the most relevant to our proposed scheme is the one presented in [2]. Motivated by this, we will next compare this detection method with the proposed one.

There are two eigenvalue-based detectors proposed in [2], of which the decision metrics are

$$\frac{\max_i\lambda_i}{\min_j\lambda_j}\quad\text{and}\quad\frac{\frac{1}{N}\sum_{i=0}^{N-1}\lambda_i}{\min_j\lambda_j}, \tag{17}$$

respectively, where $\lambda_{i,\ \{i=1,\dots N\}}$ is the i^{th} eigenvalue of the covariance matrix. While our method measures the off-diagonal power of the covariance matrix, the decision metrics in (17) are based on the ratio of the maximum eigenvalue to the minimum, and that of the average eigenvalue to the minimum, respectively. Although (17) can be extended to OFDM systems, it is shown in [14] that null subcarriers and fading channels can cause the covariance matrix to be rank-deficient, which means some eigenvalues would be zero or close to zero. Obviously, in this situation, the detection results will be unreliable since decision metrics in (17) apply the minimum eigenvalue as denominators, which can result in numerical instability.

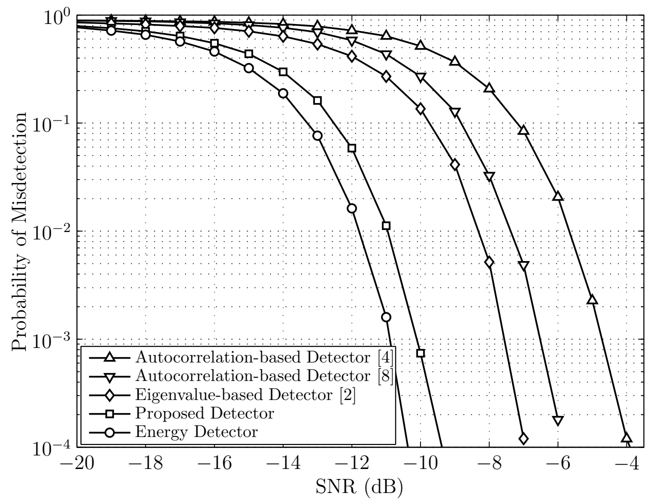

Fig. 1. P_{md} of the comparative algorithms over the AWGN channel.

V. NUMERICAL RESULTS

We consider a scenario similar to the IEEE 802.11a standard, i.e., $N=64$ and $N_g=16$. The normalized CFO is evenly distributed over $(-0.5,0.5]$, and the perfect timing is assumed. We consider the AWGN and frequency-selective channels, including the SUI-3 and SUI-4 models [15]. Source symbols are modulated using quadrature phase-shift keying (QPSK). The observation window contains 50 symbols. The energy detector (ED), the eigenvalue-based detector (EBD) [2], and two autocorrelation-based detectors (ABD) [4][8] are simulated for performance comparison with respect to the proposed scheme. The ED assumes perfect knowledge of the noise variance and, therefore, its performance is optimal and offers a baseline for comparison.

Fig. 1 demonstrates the probability of misdetection P_{md}, which is defined as $P_{md}=1-P_d$, over the AWGN channel where P_{fa} is set to 10%. The null subcarriers with indices $\{3\sim 4\}$ and $\{61\sim 62\}$ are used to estimate the noise variance for the proposed method. It's not surprising that the ED performs the best but would see a severe performance loss in the presence of a noise uncertainty. Except for the ED, the proposed method provides a better performance than the other algorithms, while the ABD in [4] is subjected to the highest error probability since the correlation incurred by the CP that this algorithm relies on could be destroyed by the CFO. For instance, the performance gain of our scheme over the EBD and the two ABDs is about 2.5 dB, 3.8 dB and 5.5 dB, respectively, at $P_{md}=10^{-3}$. Although it is possible that the other methods could include more symbols in the observation window to achieve a lower P_{md}, it is disadvantageous in situations where the sensing time requirement is stringent.

Fig. 2 and Fig. 3 show the P_{md} of different algorithms over SUI-3 and SUI-4 channels, separately, the P_{fa} is also set to 10%. The fact that all the five methods witness a

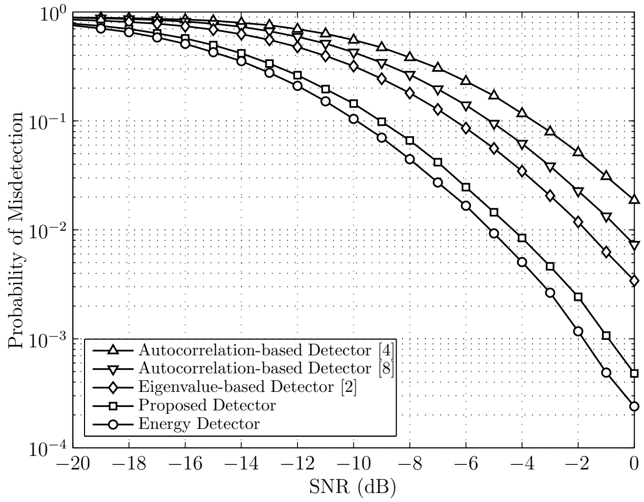

Fig. 2. P_{md} of the comparative algorithms over the SUI-3 channel.

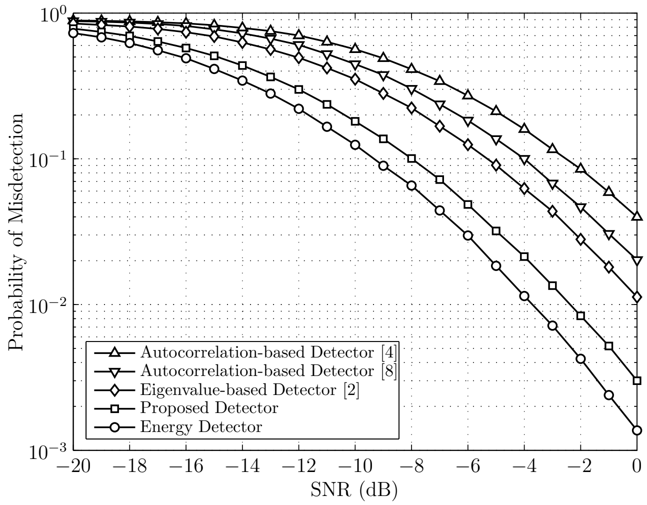

Fig. 3. P_{md} of the comparative algorithms over the SUI-4 channel.

lower P_{md} over SUI-3 than SUI-4 demonstrates the frequency selectivity of the multipath channel has a negative effect on spectrum sensing. As before, both Fig. 2 and Fig. 3 confirm that the proposed algorithm is superior over EBD and ABDs in the sense that it always has the lowest P_{md} over the whole SNR range except for the ED. The performance of EBD may suffer from rank-deficient covariance matrix caused by channel nulls. Besides, ABDs in [4] and [8] are subjected to further performance loss because the correlation incurred by the CP is further destroyed by the multipath fading. However, the EBD is more robust to the frequency offset than two ABDs.

Fig. 4 plots the receiver operating characteristic (ROC) curves of different methods over SUI-4 channel where $\mathrm{SNR} = -10$ dB. As can be observed from the figure, except for the ED, the proposed algorithm has the optimal curve where P_d increases notably with little increase of P_{fa}, especially when P_{fa} is small. On the other hand, the EBD is superior over two ABDs as the EBD's decision metric is more robust to the channel fading and CFO than that of two ABDs.

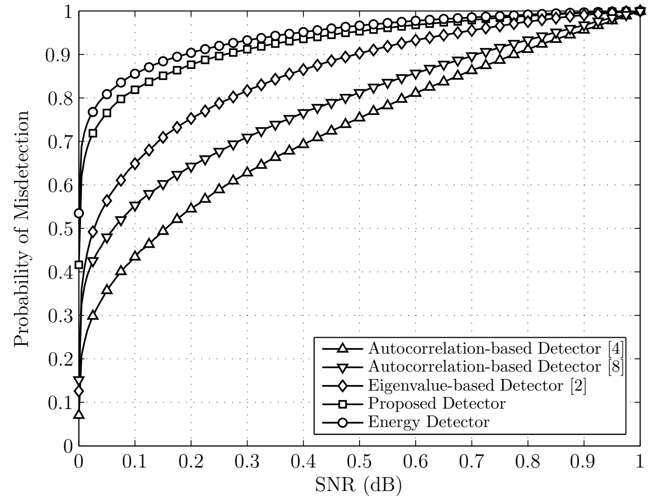

Fig. 4. ROC curves of the comparative algorithms over the SUI-4 channel.

VI. Conclusion

This paper proposed a new spectrum sensing algorithm for OFDM signals contaminated by the CFO in CR systems. This scheme is of high bandwidth utilization as it requires no training symbols or pilot tones. A new decision metric was introduced to measure the off-diagonal power of the signal covariance matrix. Given the predefined P_{fa}, we derived the threshold which depends on the number of subcarriers N, the length of symbols M and the noise variance. It was shown both theoretically and numerically that the proposed sensing is robust to the CFO, which makes it practical for real applications. Moreover, although the proposed algorithm is designed for use in scenarios with frequency offsets, it still works in the absence of this error. Numerical simulation results demonstrated that the proposed scheme outperforms several existing methods in terms of the probability of misdetection.

Acknowledgment

This work was supported by the NSFC of China under Grant 61201177.

Appendix A
Derivation of the PDFs in (10) and (13)

The detector's input is $r_{i,n} = w_{i,n}$ under $\mathcal{H}_0$, thus the $(p,q)^{th}$ off-diagonal element of the covariance matrix is $\hat{\mathbf{R}}(p,q) = \frac{1}{M}\sum_{i=0}^{M-1} W_{i,p}W_{i,q}^{*}$. According to the CLT, $\hat{\mathbf{R}}(p,q)$ is Gaussian distributed if M is large enough. Therefore, the decision metric ζ in this situation is essentially the sum of K i.i.d. distributed Rayleigh random variables, of which the PDF is approximated as

$$p(\zeta|\mathcal{H}_0) \approx \frac{1}{\sqrt{2\pi}} e^{-\frac{1}{2}\left(\frac{\zeta-\mu_{\mathcal{H}_0}\sqrt{K}}{\sigma_{\mathcal{H}_0}}\right)^2} + f_e(\zeta), \qquad \text{A.1}$$

where $\mu_{\mathcal{H}_0}$ and $\sigma_{\mathcal{H}_0}^2$ are the mean and variance of $|\hat{\mathbf{R}}(p,q)|$, respectively. $f_e(\zeta)$ compensates for the error of approximation when K is small. Since $K = \left(N^2 - N\right)/2$ is usually a large number, $f_e(\zeta)$ can be ignored. Given $\mu_{\mathcal{H}_0} = \sqrt{\frac{\pi}{4M}}\sigma_n^2$ and $\sigma_{\mathcal{H}_0}^2 = \left(1 - \frac{\pi}{4}\right)\sigma_n^4/M$, we can obtain (10).

As for (13), the corresponding $(p,q)^{th}$ entry of the sample covariance matrix is given by

$$\hat{\mathbf{R}}(p,q) \approx \frac{1}{M}\sum_{i=0}^{M-1}\Big[W_{i,p}H_{i,q-\varepsilon}^{*}X_{i,q-\varepsilon}^{*} + W_{i,q}H_{i,p-\varepsilon}^{*}X_{i,p-\varepsilon}^{*} + W_{i,p}W_{i,q}^{*}\Big]. \quad \text{A.2}$$

$\hat{\mathbf{R}}(p,q)$ can be approximated as a complex Gaussian variable if M is large enough, with its mean and variance being $\mu = 0$ and $\sigma^2 \approx (\sigma_n^4 + 2\sigma_n^2\sigma_H^2)/M$, where σ_H^2 is the variance of the channel frequency response. Therefore, ζ under $\mathcal{H}_1$ in this scenario is a sum of multiple i.i.d. Rayleigh variables. With the results in [10] and [16, pp. 295], (13) can be obtained.

Appendix B
Derivation of the PDF in (14)

In the presence of CFO, the k^{th} output of the i^{th} OFDM symbol after DFT is (6). The variance of $\hat{\mathbf{R}}(p,q)$ is approximated by σ_n^4/M as the detector often operates at $\mathrm{SNR} \ll 0$ dB. As for the calculation of the mean, the components contributed are presented by

$$\mathrm{E}\left\{\hat{\mathbf{R}}(p,q)\right\} = \mathrm{E}\left\{\sum_{t=0}^{N-1} I_{t-p}^{\varepsilon} I_{l-q}^{\varepsilon\,*} |H_{i,t}|^2\right\}. \quad \text{B.1}$$

The other components in $\hat{\mathbf{R}}(p,q)$ are ignored due to a zero mean. It can be verified that

$$\sum_{p=0}^{N-1}\sum_{q=0,p\neq q}^{N-1}\sum_{t=0}^{N-1} I_{t-p}^{\varepsilon} I_{t-q}^{\varepsilon\,*} = N\left(\left|\sum_{n=0}^{N-1} I_n^{\varepsilon}\right|^2 - \sum_{n=0}^{N-1}|I_n^{\varepsilon}|^2\right). \quad \text{B.2}$$

The mean of (B.2) can be obtained with numerical methods by integrating over $\varepsilon \in (-0.5, 0.5]$, which is $\frac{4\pi^2\sigma_H^2 N}{(\Gamma+\psi(N))^2+\psi(1,N)-\pi^2/6}$. Then the amplitude $|\hat{\mathbf{R}}(p,q)|$ in this case is Ricean distributed because of the nonzero mean. Again, since the decision metric is the sum of Ricean variables, the PDF in the presence of the primary user's signal can be approximated as [10]

$$p(\zeta|\mathcal{H}_1) \approx \frac{1}{\sqrt{2\pi}} e^{-\frac{1}{2}\left(\frac{\zeta-\mu_{\mathcal{H}_1}\sqrt{K}}{\sigma_{\mathcal{H}_1}}\right)^2}, \quad \text{B.3}$$

where $\mu_{\mathcal{H}_1} = \sigma\sqrt{\pi/2}\, L_{1/2}\left(-\mu^2/2\sigma^2\right)$ and $\sigma_{\mathcal{H}_1}^2 = 2\sigma^2 + \mu^2 - \frac{\pi\sigma^2}{2}L_{1/2}^2\left(-\mu^2/2\sigma^2\right)$. Up to this point, (14) can be obtained.

References

[1] T. Yucek and H. Arslan, "A survey of spectrum sensing algorithms for cognitive radio applications," *IEEE Commun. Surveys Tutorials*, vol. 11, no. 1, pp. 116-130, First Quarter, 2009.

[2] Y. Zeng and Y.-C. Liang, "Eigenvalue-based spectrum sensing algorithms for cognitive radio," *IEEE Trans. Commun.*, vol. 57, no. 6, pp. 1784-1793, Jun. 2009.

[3] E. Axell, G. Leus, and E. G. Larsson. "Overview of spectrum sensing for cognitive radio," in *Proc. of the International Workshop on Cognitive Information Processing*, Elba Island, Italy, Jun. 2010, pp. 322-327.

[4] Z. Lei, F. Chin, and P. S. Chin, "Sensing OFDM systems under frequency-selective fading channels," *IEEE Trans. Veh. Technol.*, vol. 59, no. 4, pp. 1960-1968, May 2010.

[5] S. Bokharaiee, H. H. Nguyen, and E. Shwedyk, "Blind spectrum sensing for OFDM-based cognitive radio systems, " *IEEE Trans. Veh. Technol.*, vol. 60, no. 3, pp. 858-871, Mar. 2011.

[6] H.-S. Chen, W. Gao, and D. G. Daut, "Spectrum sensing for OFDM systems employing pilot tones," *IEEE Trans. Wireless Commun.*, vol. 8, no. 12, pp. 5862-5860, Dec. 2009.

[7] H.-S. Chen and W. Gao, "Spectrum sensing for TV white space in North America, " *IEEE J. Select. Areas Commun.*, vol. 29, no. 2, pp. 316-326, Feb. 2011.

[8] Z. Chen, T. Luan, and X. D. Zhang, "Sensing orthogonal frequency division multiplexing systems for cognitive radio with cyclic prefix and pilot tones," *IET Comm.*, vol. 6, no. 1, pp. 97-106, Jan. 2012.

[9] Y. H. Zeng, Y.-C. Liang, and T.-H. Pham, "Spectrum sensing for OFDM signals using pilot induced auto-correlations," in *IEEE J. Select. Areas Commun.*, vol. 31, no. 3, pp. 353-363, Mar. 2013.

[10] J. A. Lopez-Salcedo, "Simple closed-form approximation to ricean sum distributions," *IEEE Signal Process. Lett.*, vol. 16, no. 3, pp. 153-155, Jun. 2009.

[11] S. M. Kay, *Fundamentals of Statistical Signal Processing, Detection Theory*. Upper Saddle River, NJ: Prentice Hall, 1993.

[12] Y. H. Zeng, S. W. Oh, and R. H. Mo, "Subcarrier sensing for distributed OFDMA in powerline communication," in *Proc. IEEE Int. Conf. Communications*, Dresden, Germany, Jun. 2009, pp. 1-5.

[13] M. Speth, S. A. Fechtel, G. Fock, and H. Meyr, "Optimum receiver design for wireless broad-band systems using OFDM-Part I," *IEEE Trans. Commun.*, vol. 47, no. 11, pp. 1668-1677, Nov. 1999.

[14] X. Ma, C. Tepedelenlioglu, G. B. Giannakis, and S. Barbarossa, "Non-data-aided carrier offset estimators for OFDM with null subcarriers: Identifiability, algorithms, and performance," *IEEE J. Select. Areas Commun.*, vol. 19, no. 12, pp. 2504-2515, Dec. 2001.

[15] V. Erceg et al., Channel models for fixed wireless applications IEEE 802.16 Broadband Wireless Working Group, IEEE802.16a-03/01, Tech. Rep., 2003.

[16] K. Krishnamoorthy, *Handbook of Statistical Distributions with Applications*, Boca Raton, FL: Chapman and Hall/CRC, 2006.